Nonlinear Model of Epitaxial Layer Resistor on GaAs Substrate

Yu Zhu, Cejun Wei, Oleksiy Klimashov, Cindy Zhang, and Yevgeniy Tkachenko

Skyworks Solution Inc., 20 Sylvan Road, Woburn, MA 01801, USA

Abstract — **A large signal model is proposed for GaAs epitaxial layer resistor, which can be used in resistor design, characterization and circuit simulation. The resistor I-V behavior can be excellently fitted by a hyperbolic tangent expression with only two model parameters. By taking into account the nonlinearities, frequency dispersion, and parasitic effect, the proposed model accurately predicts DC, small signal S parameter, and power performances of resistors.**

I. Introduction

Epitaxial layer resistors are essential to the microwave monolithic integrated circuits. The nonlinear I-V behaviors have been reported for both polysilicon and GaAs epitaxial layer resistors. While efforts have been attributed to modeling the nonlinear behavior of polysilicon resistor [1], [2], the nonlinear behaviors of GaAs resistor have been generally ignored in the modeling for circuit simulation.

The nonlinearities are usually undesirable, which cause performance degradation and require more conservative and complicated circuit designs [3]. In some cases, however, the nonlinearities are useful in achieving better circuit performance [4], [5]. Whether it is intended to use the resistors as linear or nonlinear devices, a nonlinear resistor model is desired to examine the proper operating condition and provide accurate simulation result.

The main goal of this work is to provide a nonlinear resistor model for GaAs resistor design, characterization, and the circuit simulation. The experimental details are given in Section II, the proposed model and the model validation via DC, S parameter, and power performance are given in Section III. The study is concluded in Section IV.

II. Experiment

The resistors with ground-signal-ground test pad were fabricated on the wafers with either MESFET or HEMT epitaxial structure. Static I-V, pulse I-V, S parameter, and power measurements are performed via probe station. The model generation and validation are illustrated by an example; a resistor fabricated on the wafer with sheet resistance of 190 Ω/sq, and the length and width of the resistor are 18.75 and 8 μm, respectively.

III. Nonlinear Resistor Modeling

A. DC Behavior

GaAs resistors exhibit different nonlinearities from those of polysilicon resistors. The resistor current saturates, and thus the resistance increases with increasing voltage. Current saturation of GaAs resistor is the result of the carrier velocity saturation. Because of the low saturation field in GaAs (3kV/cm) [6], the current saturation can be observed under certain low voltage condition for short length GaAs resistors.

By regarding the epitaxial layer resistor as a FET without gate electrode, it is understandable that the resistor I-V behavior can be described by a FET channel current model. By simplifying the Materka-Kacprzak FET model [7], a nonlinear resistor model is proposed as

$$I = I_S \tanh\left(\frac{V}{R_0 I_S}\right) \qquad (1)$$

where I_S is the saturation current, and R_0 the linear resistance in the linear region, they are the only two model parameters needed and easy to be extracted. The comparison of measured and modeled DC I-V characteristics is shown in Fig. 1. The simple expression accurately represents the nonlinear I-V behavior in the entire voltage region, and the parameters extracted are R_0=518Ω and I_S =8.48mA. The parameter I_S can be considered as a measure of the nonlinearity. The smaller the I_S, the stronger the nonlinearity.

(1) reduces to the linear expression

$$I = V / R_0 \qquad (2)$$

for V<< $R_0 I_S$. If (2) is used to extract R_0, attention should be paid to the voltage range within which the extraction is performed. Figure 2 shows the voltage range dependence of the R_0 extracted with (1) and (2), respectively. While the R_0 extracted using (1) keeps almost constant, the R_0 using (2) depends sensitively on the voltage range. Therefore even a linear resistor model is used in simulation, more reliable model parameter R_0 can be obtained by using (1) instead of (2).

The differential resistance can be obtained by differentiating (1) as

$$R = R_0 \cosh^2\left(\frac{V}{R_0 I_S}\right) \qquad (3)$$

(3) predicts the increase in differential resistance with increasing the voltage, and is useful for calculating the differential resistance at any specified voltage. The comparison of measured and modeled DC differential resistance, shown in Fig. 3, further confirms the accuracy of the proposed model.
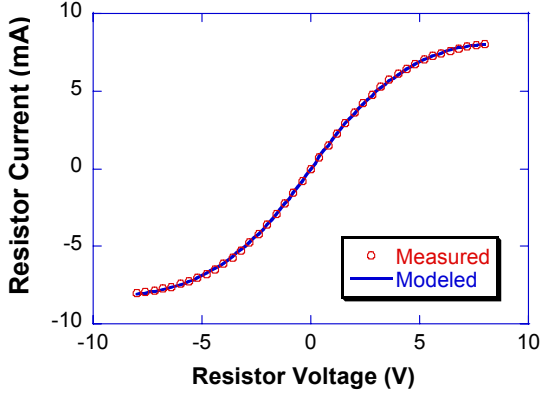
Fig. 1. Measured and modeled resistor I-V characteristics.
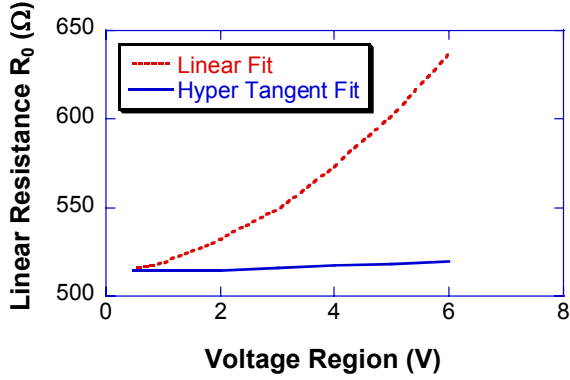
Fig. 2. Comparison of R_0 extracted by using (1) and (4).
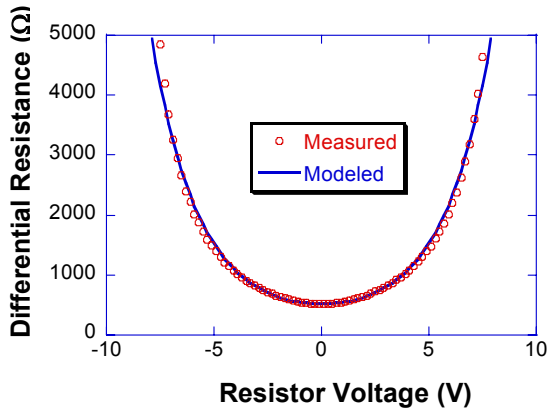
Fig. 3. Measured and modeled differential resistance.

	DC	RF
$R_0\,(\Omega)$	518	523
$I_S\,(mA)$	8.48	10.8

TABLE I
MODEL PARAMETERS FROM DC AND RF MEASUREMENTS

If a linear region is defined in terms of the change in differential resistor ΔR, the corresponding voltage limit can be obtained from (3) as

$$V_{max} = R_0 I_S \cosh^{-1}(\sqrt{1 + \Delta R / R_0})\qquad(4)$$

With $\Delta R/R_0=10\%$, we have Vmax=1.36V for the $8\times18.75\mu m^2$ resistor measured. The corresponding electrical field is 0.7kV/cm, which is much lower than the saturation field in GaAs. Linear region should be examined when a linear resistor model is going to be used.

B. Frequency Dispersion

The two model parameters Is and R_0 have also be extracted from the S parameter measured at different voltage. The parameters extracted from DC and S parameter behaviors are summarized in Table I. The frequency dependence of the parameters, namely the frequency dispersion, can be observed. It is believed that the frequency dispersion is due to the deep carrier traps and the thermal effect as reported for GaAs FET [8]. The frequency dispersion can also be observed in terms of pulse response as shown in Fig. 4.

Figure 5 shows the equivalent circuit of the resistor model. In order to describe the frequency dispersion, two current sources, Idc and Irf, are used to represent the DC and RF behaviors, respectively. By connecting the current sources with a capacitance and an inductance as shown in Fig. 5, the Idc (Irf) become dominant in the frequency range of $f \ll 1/2\pi\sqrt{LC}$ ($f \gg 1/2\pi\sqrt{LC}$). The inductance Ls is used to represent the parasitic inductance especially for long length resistors.
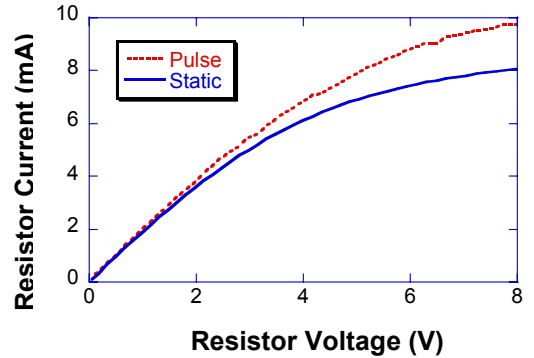
Fig. 4. Static and pulse I-V characteristics.
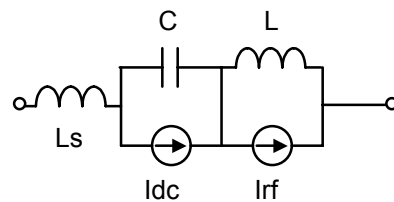
Fig. 5. Equivalent circuit of resistor model.
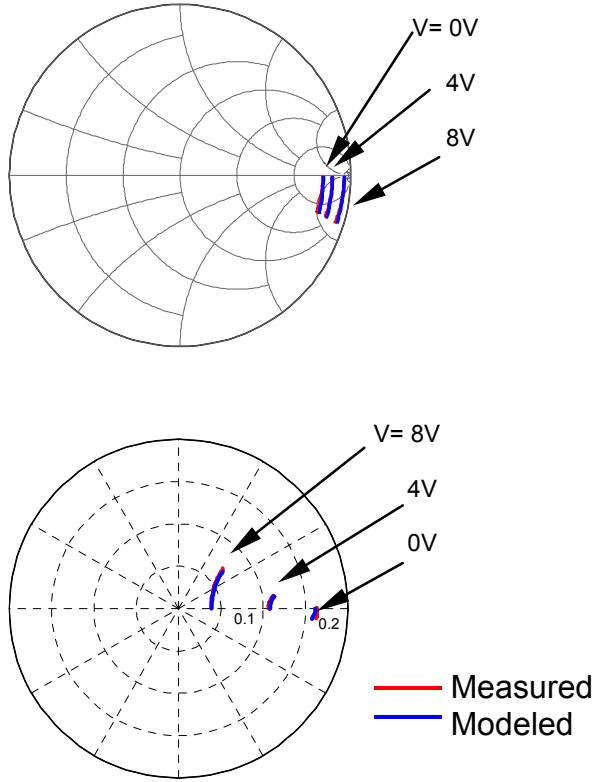
Fig. 6. Measured and modeled (a) S11, (b) S12.

Figure 6 shows the measured and the model S parameter. The frequency range for the measurement and the simulation is form 0.2 to 20.2 GHz. Since the model parameters can be adjusted independently for Idc and Irf, the DC and S parameter fitting can easily be achieved.

C. Power Performances

The model developed was further verified through power behaviors. The single tone measurements were performed at the fundamental frequency of 2400MHz. Figure 7 (a) shows the comparison of the measured and modeled single tone behaviors at bias voltage of 0V. The good agreements between the measured and modeled results are achieved for fundamentals and the third harmonic waves. Since (1) is an odd function at V=0V, no even harmonic waves appear in the simulation result. Since it is difficult to fabricate a perfect symmetric resistor, the real I-V behavior is probably not an exact odd function at V=0. The measured 2nd harmonic, which is much lower than the 3rd harmonic, can be regarded as a measure of the device asymmetry.

Figure 7 (b) shows the comparison of the measured and modeled single tone behaviors at bias voltage of 4V. Since (1) is no longer an odd function at V=4V, 2nd harmonic wave, which is much higher than the 3rd harmonic, were observed in both simulation and measurement. Agreements are achieved for fundamental, 2nd, and 3rd harmonic waves.

Figure 8 shows the input power dependence of DC currents. The current decreases with increasing input power at V=4V, which can be explained with the current saturation. The good match between the measured and modeled DC currents can be observed. It is concluded
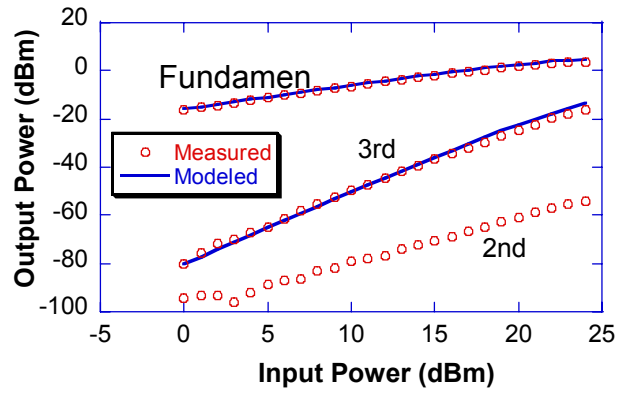
(a)
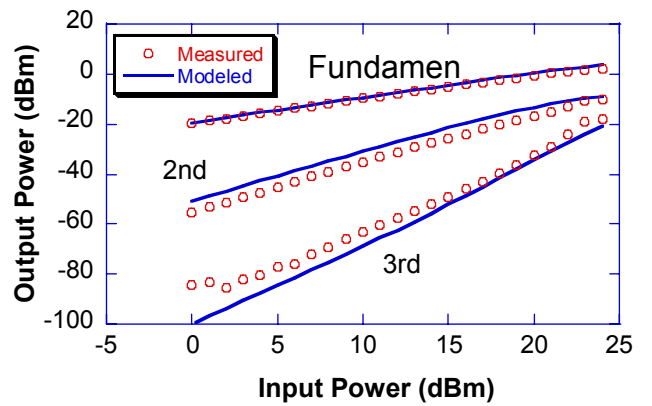
(b)

Fig. 7. Comparison of measured and modeled single-tone power performances, (a) V=0V, (b) V=4V.
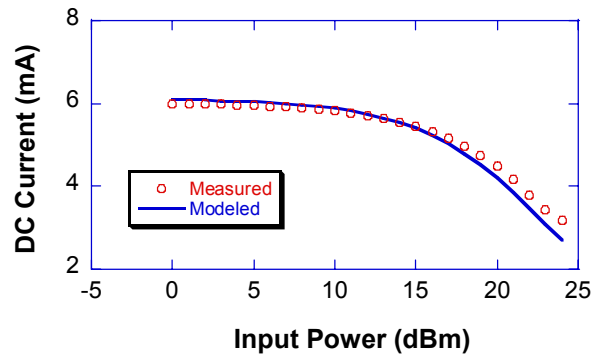
Fig. 8. Measured and modeled DC current versus input power.
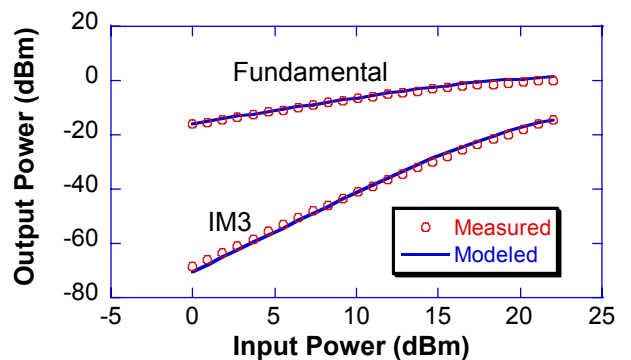
Fig. 9. Measured and modeled inter-modulation performances.

that the proposed model accurately predicts both DC and high frequency large signal performances.

Figure 9 shows the inter modulation performance measured at V=0V. The frequencies used are f1=2399 and f2=2401 MHz, respectively. Good agreements have been achieved for both fundamental and the IM3. The resistor exhibits strong non-linearity with IM3 as high as 15dBc at Pin=22dBm.

While only the measured data of $8 \times 18.75 \mu m^2$ resistor have been illustrated here, the model has been verified using the resistors with various width, length, and sheet resistance.

IV. CONCLUSION

A nonlinear model has been developed for epitaxial layer resistor on GaAs substrate. The description of the nonlinear I-V behavior, the calculation of differential resistance, and the estimation of a linear region can easily be achieved based on the hyperbolic tangent expression. Frequency dispersion has been taken into account by using two current sources in the model. Excellent agreements between measured and model results have been obtained for DC, small signal S parameter, and large signal power performances. The proposed model is useful for resistor design, characterization, and circuit simulation.

ACKNOWLEDGEMENT

REFERENCES

[1] R. Virkus, D. Weiser, K. Green, D. Richardson, and G. Westphal, "Modeling of non-linear Polysilicon resistors for analog circuit design," Proc. IEEE Int. Conf. on Microelectronic Test Structures, vol. 14, no. 12, pp. 89-91, March 2001.

[2] N. C. C. Lu, L. Gerzberg, C. Y. Lu, and J. D. Meindl, "Modeling and optimization of monolithic polycrystalline silicon resistors," IEEE Trans. Electron Devices, vol. ED-28, no. 7, pp. 818-830, July 1981.

[3] K. Honjo, T. Sugiura, and H. Itoh, "Ultra-broad-band GaAs monolithic amplifier," IEEE Trans. Microwave Theory & Tech, vol. 28, no. 7, pp. 1027-1033, July 1982.

[4] C. P. Lee, B. M. Welch, and R. Zucca, "Saturated resistor load for GaAs integrated circuits," IEEE Trans. Microwave Theory & Tech, vol. 28, no. 7, pp. 1007-1013, July 1982.

[5] J. Jang, E. C. Kan, T. Arnborg, T. Johansson, and R. W. Dutton, "Characterization of RF power and improvement of thermal stability with nonlinear base ballasting," IEEE J. Solid-State Circuit, vol. 33, no. 9, pp. 1428-1432, Sept., 1998.

[6] P. A. Houston and A. G. R. Evans, "Electron drift velocity in n-GaAs at high electric fields," Solid-State Electron., vol. 20, pp. 197-204, Sept., 1977.

[7] A. Materka and T. Kacprzak, "Computer calculation of large-signal GaAs FET amplifier characteristics," IEEE Trans. Microwave Theory & Tech, vol. 33, no. 2, pp. 129-135, Feb., 1985.

[8] A. E. Parker, and J. G. Rathmell, "Novel technique for determining bias, temperature and frequency dependence of FET characteristics," 2002 IEEE MTT-S Int. Microwave Symp. Dig., vol. 2, pp. 993-996, June 2002.